

State Dependent Parameter Modelling of a DC-DC Boost Converter in Discontinuous Conduction Mode

U. Hitzemann¹ and K. J. Burnham^{1,2}

¹Control Theory and Applications Centre, Coventry University, Coventry, U.K.

²Faculty of Electronics, Wroclaw University of Technology, Wroclaw, Poland

Keywords: DC-DC Boost Converter, Nonlinear Circuits, State-dependent Parameter Modelling, System Identification, System Modelling.

Abstract: This paper is concerned with the modelling of a DC-DC boost converter, operating in discontinuous conduction mode (DCM). The approach chosen is to model the converter using a state-dependent parameter (SDP) model approach which is expected to be able to deal with the nonlinearities of the system, as well as a varying load. The modelling procedure presented, makes use of input-output data only and no physical insight into the system is required. Results are verified via laboratory experiments.

1 INTRODUCTION

DC-DC boost converters are switched mode power electronic devices. The boost converter steps up a DC input voltage to a higher DC output voltage. Hence they find their application where a higher, controlled DC voltage than the supply voltage is required; this being the case, e.g. in DC-motor drive applications or power distribution systems.

The difficulty in modelling a DC-DC converter lies in its hybrid nature due to the switching process. There are two conditions which are required to be considered, namely, when the switch is open and when the switch is closed. In discontinuous conduction mode (DCM), an additional condition of the converter is required to be taken into account, i.e. when the switch is open and the inductor is not conducting.

In the literature, the common approach used to model a DC-DC converter is the state-space averaging method (Middlebrook and Cuk, 1976; Erickson and Maksimovic, 2001; Sun et al., 2001; Xie et al., 2010), where each of the conditions are modelled separately and the models are averaged over the entire period. The models are usually obtained by making use of physical relationships. Often, however, an exact physical insight into the converter is not necessarily available, due to the tolerances of the components and their inherent parasitic elements. The approach considered in this paper requires no physical insight since the modelling process makes use of the input - output data only. Additionally, the 'linear-like' struc-

ture of the state-dependent parameter (SDP) model (see (Young, 2000)) makes it suitable in the design of model based controllers, allowing linear control theory to be used. This is not necessarily the case when making use of models based on physical relationships. In several practical systems, model based control, such as the proportional integral plus controller (PIP), based on SDP models has already been successfully applied (Taylor et al., 2007). All results presented here are verified via experiments using a practical, laboratory based DC-DC boost converter.

The paper is organised as follows: A brief description of the boost converter is given in Section 2. The SDP model of the converter is obtained in Section 3. Conclusions are given in Section 4.

2 DC-DC BOOST CONVERTER

In this Section, the boost converter is briefly introduced. Figure 1 shows the topology of a boost converter with ideal components, where L , C , S and R denote the inductor, the capacitor, the switch and the load represented by a resistor, respectively. The quantities V_i , V_o , v_L and v_C denote the input voltage, the output voltage, the voltage across the inductor and the voltage across the capacitor, respectively. The switch, represented by a MOSFET, is driven by a pulse-width-modulated (PWM) voltage with a duty-

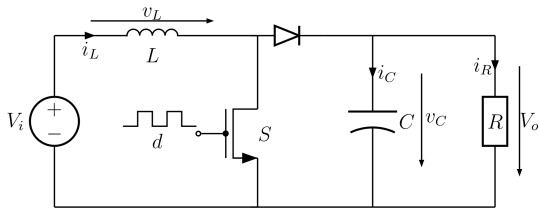


Figure 1: Topology of a DC-DC boost converter with ideal components.

cycle, denoted d , which is defined as

$$d = \frac{T_{on}}{T_s} \quad (1)$$

where $T_s = T_{on} + T_{off}$ denotes the period of the PWM signal. The time interval, denoted T_{on} , when the PWM signal is high, corresponds to the switch conducting, while T_{off} corresponds to the time interval when the PWM signal is low and to the switch not conducting.

Additionally, the duty-cycle of a PWM signal can only vary between 0% and 100% so that d is defined to be in the per-unit range

$$\{d \in \mathbb{R} \mid 0 < d \leq 1\} \quad (2)$$

In the following, a brief description of the principle of operation is provided. The inductor and the capacitor are energy storage components. When the switch is closed, during T_{on} , the inductor is charged and only the capacitor supplies the load while the diode ensures that no current is able to flow from the capacitor via the switch to ground, i.e. a short circuit across the capacitor. When the switch is open, during T_{off} , the energy stored in the inductor is transferred to the capacitor and to the load. Consequently, when considering the law of energy conservation, it can be concluded that the output voltage V_o can be influenced by the duty-cycle of the PWM signal. For detailed information, see e.g. (Erickson and Maksimovic, 2001).

2.1 Operational Modes

In general, the converter either operates in continuous conduction mode (CCM) or in DCM. However, the latter is considered in this paper only. The difference is that in CCM, the inductor current is always greater than zero, as shown in Figure 2, where the inductor continuously conducts current. In DCM, the inductor current settles to zero and remains at this value until the end of the period. This time interval is denoted by T_z .

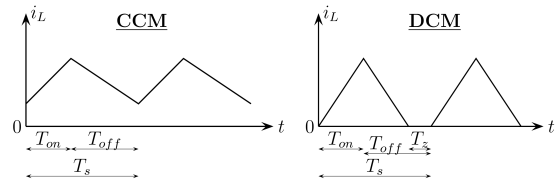


Figure 2: Idealised inductor current in CCM and in DCM.

2.2 Converter Set-up

The set-up of the prototype converter used for laboratory experiments is as follows: $V_i = 5\text{ V}$, $L = 745\ \mu\text{H}$ with inherent series resistance of $\approx 1.3\ \Omega$ and $C = 1\ \text{mF}$. For DCM operation, the switching period, which is also equivalent to the sampling interval, is chosen to be $T_s = 1\ \text{ms}$. In order to generate the PWM signal and to obtain the required measurements, the dSPACE MicroAutobox DS1401 is used. The maximal measurable output voltage V_o is limited to $V_o = 20\ \text{V}$, hence the output voltage is defined to be in the range

$$\{V_o \in \mathbb{R} \mid 5\ \text{V} \leq V_o \leq 20\ \text{V}\} \quad (3)$$

The maximum current, which can be delivered by the power supply is limited, hence the value $i_L = 2\ \text{A}$ cannot be exceeded.

The load, represented by R in Figure 1, is realised as shown in Figure 3. This allows the output current i_R to be determined by applying a load reference voltage V_{ref} . This is provided by the DS1401 digital to analog converter. The resistor $R_{Io} = 10\ \Omega$ is assumed to be accurately known. The operational amplifier regulates the resistance of the transistor via $R_T = 220\ \Omega$ in such a way, that the voltage across the resistor R_{Io} is equal to V_{ref} and the output current is given by $i_R = \frac{V_{ref}}{R_{Io}}$ provided that the base current $i_B \ll i_R$, so that $i_R = i_{R_{Io}}$.

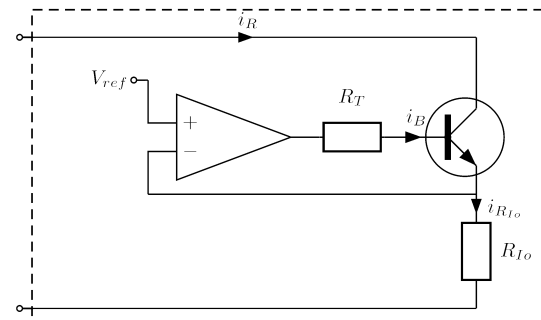


Figure 3: Realisation of the load R (dashed box).

Realising the load in this way, provides the opportunity of considering different loading scenarios.

Due to the above mentioned hardware limitations, and in order to ensure DCM operation, the output current is defined to be in the range

$$\{i_R \in \mathbb{R} \mid 40 \text{ mA} \leq i_R \leq 140 \text{ mA}\} \quad (4)$$

3 SDP – MODEL

The converter is referred to in the following as the system, and the modelling approach is based on measured input-output data. These are obtained by applying a staircase input signal to the system of an appropriate step height. Furthermore, the output current is kept constant during each staircase response. Then, the output current is incremented and the procedure is repeated. The value of the output current starts at $i_R = 40 \text{ mA}$ and is incrementally increased to 140 mA in steps of 10 mA . The input step height in each staircase response is required to be chosen appropriately in order to obtain sufficient step responses, covering the entire operating range. An exemplary yet representative staircase input and corresponding measured output voltage are shown in Figure 4, when $i_R = 100 \text{ mA}$. Based on these input-output data, the modelling procedure is performed.

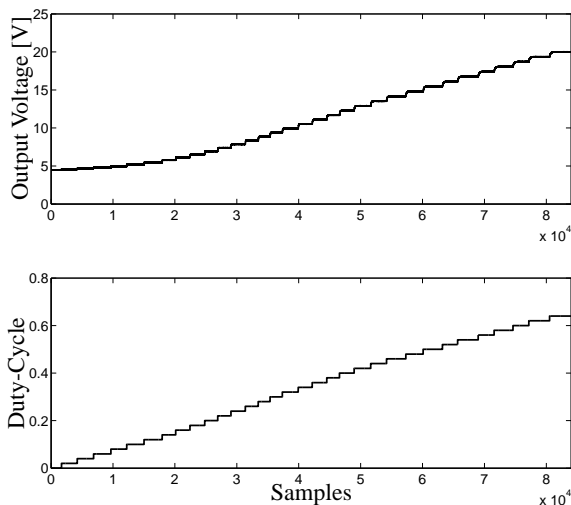


Figure 4: Measured output voltage response (upper) to the staircase input signal (lower) with constant output current value of $i_R = 100 \text{ mA}$.

3.1 SDP structure

Consider the following system equation

$$\begin{aligned} y_k + a_1(s_k)y_{k-1} + \dots + a_{n_a}(s_k)y_{k-n_a} \\ = b_1(s_k)u_{k-1} + \dots + b_{n_b}(s_k)u_{k-n_b} \end{aligned} \quad (5)$$

where y_k and u_k denote the system output voltage and system input, i.e. the duty-cycle, respectively.

s_k indicates, that the parameters are functions of one or more elements of the non-minimal state vector (Young et al., 1987; Wang and Young, 1988), i.e. system output voltage and system input, and/or functions of other variables, see (Young, 2000).

In addition, by adopting the SDP model structure (5), the ‘frozen’ linear system, as defined by the SDP model at every sampling instant, can form the basis for state dependent control system design based on linear control methods (Kontoroupi et al., 2003). However, global stability cannot be guaranteed if there is model mis-fit (Taylor et al., 2009) and so the closed loop system must be investigated carefully in this regard.

3.2 System Identification

From the staircase responses, as shown in Figure 4, and, in particular, the individual steps of the staircase, as shown in Figure 5, it can be concluded that a first order system model is an adequate choice, i.e. $n_a = n_b = 1$. This means, that only the parameters $a_1(s_k)$ and $b_1(s_k)$ are required to be identified.

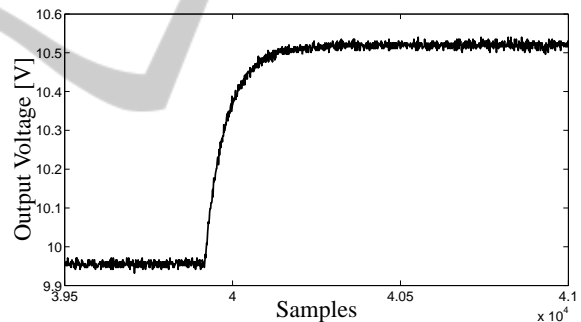


Figure 5: Magnified single step of the staircase response shown in Figure 4.

Initially, the steady-state behaviours for each output current are modelled. The function, which describes the steady-state behaviours is found empirically to be of the polynomial form

$$y_{j,\infty}(u_\infty) = \sum_{l=1}^4 \beta_{j,l} u_\infty^{4-l} \quad (6)$$

where $j = 1, 2, \dots, 10$, which corresponds to the output currents $i_R = 40 \text{ mA}, 50 \text{ mA}, \dots, 140 \text{ mA}$. $y_{j,\infty}$ and u_∞ denote the steady-state output and input, respectively. The parameters $\beta_{j,l}$ are identified by making use of the least-squares algorithm, see e.g. (Hsia, 1977). At this point, it is noted that the parameters $\beta_{j,l}$ can be formulated as functions of the output current. Again, the function is found empirically to be of

the polynomial form

$$\beta_l(i_R) = \sum_{f=1}^4 \gamma_{l,f} i_R^{4-f} \quad l = 1, 2, \dots, 4 \quad (7)$$

where i_R is in mA. The constant parameters $\gamma_{l,f}$ are identified, by making use of the least-squares method. Substituting (7) into (6) yields the modelled steady-state behaviour of the system that is dependent on the output current

$$y_\infty(i_R, u_\infty) = \sum_{l=1}^4 \beta_l(i_R) u_\infty^{4-l} \quad (8)$$

The steady-state output against the steady-state input is shown in Figure 6, where each trace, from left to right, corresponds to the output currents of fixed value $i_R = 40 \text{ mA}, 50 \text{ mA}, \dots, 140 \text{ mA}$. The steady-state behaviour obtained from measurements are compared against the identified polynomials (6) (solid lines) and against the polynomial where the coefficients are modelled as output current dependent quantities (8) (dashed line). It can be observed, that the mismatch at high output currents and high voltages increases. Figure 7 shows the parameters obtained from (6) (solid line) and the estimated, output current dependent parameters according to (7) (dashed line).

Having characterised the steady-state behaviour, the next step is to consider the transients, and the system parameter $a_1(s_k)$ is required to be identified. Since this parameter is not measurable directly, each step of each staircase response is considered individually. Here, a first order linear model of the form (5), but with invariant parameters, is identified by making use of the least-squares algorithm. In this way, $a_1(s_k)$ at several points through the entire operating range is obtained. The estimated system parameter values

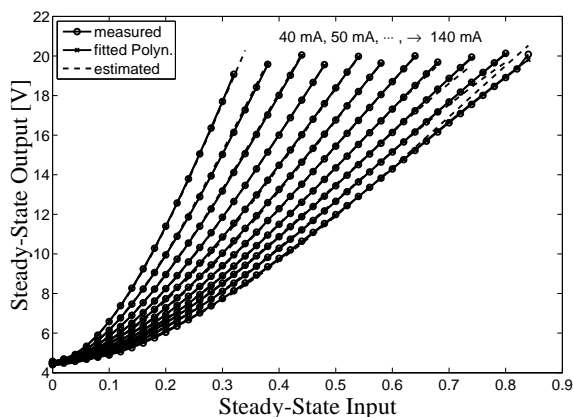


Figure 6: Steady-state behaviour, measured and modelled by fitting polynomials (solid lines) as well as modelled by a polynomial incorporating the output current (dashed line), for output currents starting at $i_R = 40 \text{ mA}$ increasing in steps of 10 mA up to $i_R = 140 \text{ mA}$, from left to right.

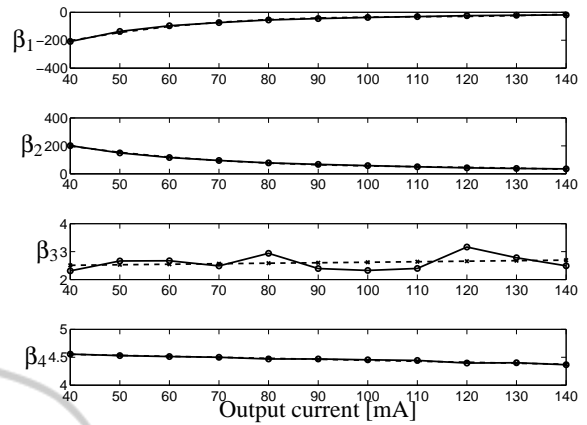


Figure 7: Parameters of (8) β_l obtained as a function of the output current (7) (dashed line) and obtained directly from considering the individual steady-state behaviours (6) (solid line).

$a_1(s_k)$ are shown in Figure 8, where each trace corresponds to the staircase responses obtained for each output current value $i_R = 40 \text{ mA}, 50 \text{ mA}, \dots, 140 \text{ mA}$. The output current dependency of the system parameter $a_1(s_k)$, which is also a measure of the time constant of the system, is not immediately obvious in the discrete time domain, as shown in Figure 8. The differences of the traces seem to be marginal, in particular with increasing output voltage. This means that since each trace corresponds to a certain constant output current, the output current dependency on the system parameter $a_1(s_k)$ would apparently appear to be insignificant. For this reason, an averaged function, independent of the output current, describing $a_1(s_k)$ was used in (Hitzemann and Burnham, 2011). This implies, that the transient behaviour of the converter does not depend on the output current significantly. However, to highlight the dependency, Figure 9 shows the time constant τ of the system against the output voltage, where, again, each trace corresponds to a certain value of the output cur-

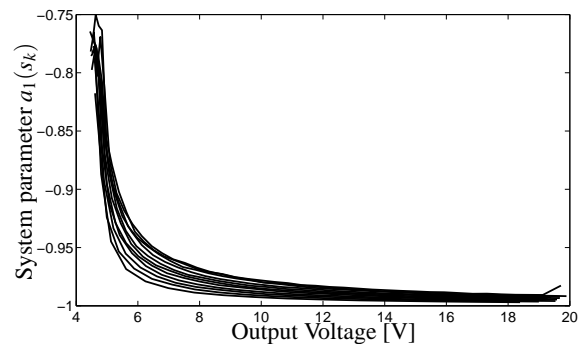


Figure 8: System parameter $a_1(s_k)$ against the output voltage where each trace corresponds to the output current values $i_R = 40 \text{ mA}, 50 \text{ mA}, \dots, 140 \text{ mA}$.

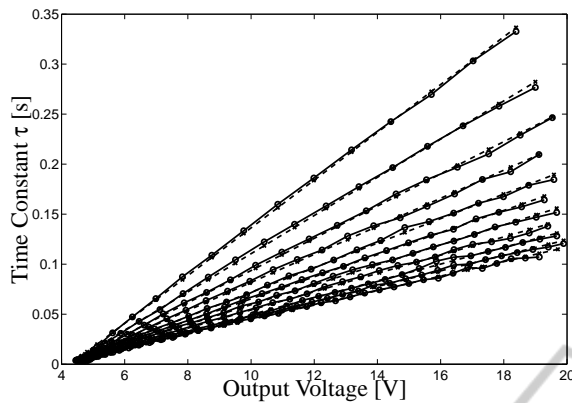


Figure 9: Time constants, obtained from staircase responses directly (solid line) and estimated (dashed line), against the output voltage. Each trace corresponds to a fixed output current $i_R = 40 \text{ mA}, 50 \text{ mA}, \dots, 140 \text{ mA}$, from upper to lower.

rent $i_R = 40 \text{ mA}, 50 \text{ mA}, \dots, 140 \text{ mA}$. Here, the output current dependency of the time constant and hence of $a_1(s_k)$ is clearly discernable. Additionally, it can be observed, that the spread of the traces increases when the output voltage increases. Hence, it can be deduced that the output current dependency of the transient behaviour does in fact increase when the output voltage increases.

Due to the approximately linear nature of the time constant with respect to the output voltage, considering a constant output current, the following function is obtained.

$$\tau_j = \alpha_{j,1} y_{\infty} + \alpha_{j,2} \quad j = 1, 2, \dots, 10 \quad (9)$$

In order to incorporate the output current dependency, the parameters $\alpha_{j,1} = \alpha_{j,1}(i_R)$ and $\alpha_{j,2} = \alpha_{j,2}(i_R)$ are assumed to be functions of the output current, cf. in a similar manner to modelling the steady-state behaviour described above

$$\alpha_f(i_R) = \sum_{l=1}^4 \eta_{f,l} i_R^{A-l} \quad f = 1, 2 \quad (10)$$

where $\eta_{f,l} \in \mathbb{R}$ are constant coefficients identified by the least-squares method. Subsequently, the system parameter $a_1(s_k)$ can be obtained by substituting (10) into (9), denoted $\tau(y_{k-1}, i_R)$, and mapping back to the discrete time domain via

$$a_1(s_k) = -e^{-\frac{T_s}{\tau(y_{k-1}, i_R)}} \quad (11)$$

The remaining system parameter $b_1(s_k)$ is required to be obtained in order to satisfy the steady-state behaviour. Consequently, this parameter is given by

$$b_1(s_k) = \frac{y_{k-1}(1 + a_1(s_k))}{y_{\infty}^{-1}(i_{R,k}, y_{k-1})} \quad (12)$$

where $y_{\infty}^{-1}(i_{R,k}, y_{k-1})$ denotes the inverse function of (8).

Remark 1. In (12), to avoid division by zero, the system output is required to be greater than that value which causes $y_{\infty}^{-1}(i_{R,k}, y_{k-1})$ to be zero, hence, the lower bound of (3) is required not to be exceeded during operation. This in turn, prevents the system input from becoming zero, which is reflected in (2).

Remark 2. In this paper, the functions used in order to describe the steady-state behaviour, (6) - (8), as well as the functions used in order to describe the dynamic behaviour, (9) and (10), are chosen to be polynomials of third and first order, respectively. Hence, the identification of the associated constant parameters is straightforward by making use of least-squares rather than requiring numerical optimisation methods as used in (Hitzemann and Burnham, 2011).

Remark 3. The presented system identification procedure linearises the system at several operating points through the entire operating range and ‘interpolation’ is invoked in between. Considering this, the incremental step height of the output current and the input steps of the staircase signal are required to be chosen with care in order to obtain sufficient accuracy of the resulting overall system model.

3.3 Model Validation

Having obtained a model of the system, an arbitrary input sequence is applied to both the system and the model, for validation purposes. An arbitrary output current is drawn from the system and applied to the model, which represents a varying load. Figure 10 shows the response of the model and the measured response of the system. It can be seen that the model is capable of replicating the system response adequately. Nevertheless, steady-state offset errors are observed, e.g. the peak between $\approx 85 \text{ s}$ and 90 s . Note that when taking the output current and the output voltage into account, which are both high, this observation is in agreement with the results shown in Figure 6.

4 CONCLUSIONS

In this paper, an approach to modelling a DC-DC boost converter in discontinuous operation mode has been presented. The state dependent parameter model structure has been selected. The presented modelling approach relies on measured input-output data only and not on the knowledge of physical relationships. However, this modelling approach requires a constant output current, independent of the output voltage, to

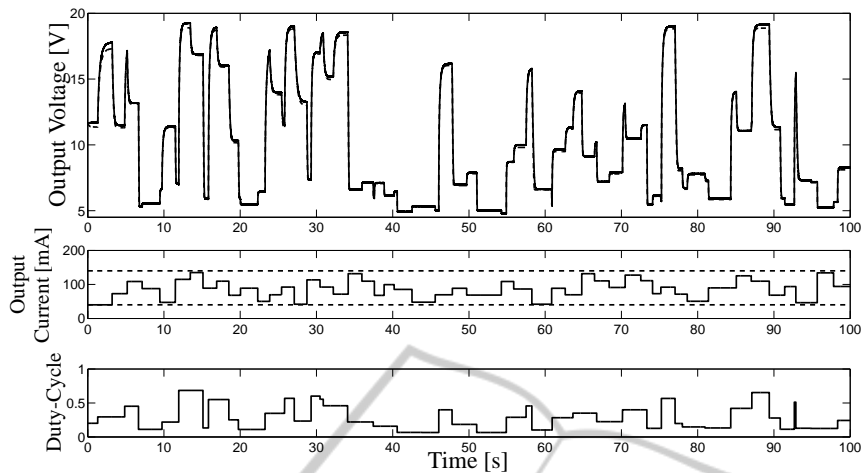


Figure 10: Upper: measured output response of the system (solid line) and output response of the model (dashed line) to arbitrary varying sequences of the input signal and output current. Middle: arbitrary varying output current sequence (solid line) in the defined range $40\text{mA} \leq i_R \leq 140\text{mA}$ (dashed lines). Lower: arbitrary varying input sequence.

be drawn from the converter, which is realised by a load as shown in Figure 3. Furthermore, the associated identification steps make use of polynomials, so that parameters can be identified straightforwardly by making use of standard system identification algorithms such as least-squares. Additionally, the transients are modelled by considering the time constants in the continuous time domain of the equivalent linear models at several operating points, which are then mapped back in the discrete time domain. In this way, the identification of the transient behaviour is also modelled in a straightforward way by making use of linear relationships. The resulting state dependent parameter model is able to deal with varying loads by taking the output current into account. Finally, the state dependent parameter model has been validated via a laboratory based experiment confirming its accuracy and appropriateness.

REFERENCES

- Erickson, R. W. and Maksimovic, M. (2001). *Fundamentals of Power Electronics*. Kluwer Academics/Plenum Publishers, New York, 2nd edition.
- Hitzemann, U. and Burnham, K. J. (2011). State dependent parameter modelling and control of a dc-dc boost converter in discontinuous conduction mode. In *Proceedings of the 9th European Workshop on Advanced Control and Diagnosis, ACD 2011*, Budapest, Hungary.
- Hsia, T. C. (1977). *System Identification: Least-Squares Methods*. Lexington Books, Massachusetts.
- Kontoroupi, P., Young, P. C., Chotai, A., and Taylor, C. J. (2003). State dependent parameter-proportional integral plus (sdp-pip) control of nonlinear systems. *Proc. 16th Int. Conf. on Systems Engineering, ICSE'2003*, pages 373–378.
- Middlebrook, R. D. and Cuk, S. (1976). A general unified approach to modelling switching-converter power stages. In *IEEE Proceedings of Power Electronics Specialists Conference*, pages 18–34.
- Sun, J., Mitchell, D. M., Greuel, M. F., Krein, P. T., and Bass, R. M. (2001). Averaged modeling of pwm converters operating in discontinuous conduction mode. *IEEE Transaction on Power Electronics*, 16(4):482–492.
- Taylor, C. J., Chotai, A., and Young, P. C. (2009). Non-linear control by input-output state variable feedback pole assignment. *International Journal of Control*, 82(6):1029–1044.
- Taylor, C. J., Shaban, E. M., Stables, M. A., and Ako, S. (2007). Proportional-integral-plus control applications of state-dependent parameter models. *Proc. IMechE Part I: Journal of Systems and Control Engineering*, 221(7):1019–1032.
- Wang, C. L. and Young, P. C. (1988). Direct digital and adaptive control by input-output state variable feedback pole assignment. *International Journal of Control*, 47(1):97–109.
- Xie, G., Fang, H., and Cheng, X. (2010). Non-ideal models and simulation of boost converters operating in dcm. *International Journal of Computer and Electrical Engineering*, 2(4):730–733.
- Young, P. C. (2000). *Nonlinear and Nonstationary Signal Processing*, chapter Stochastic, dynamic modelling and signal processing: time variable and state dependent parameter estimation., pages 74–114. Cambridge University Press, Cambridge.
- Young, P. C., Behzadi, M. A., Wang, C. L., and Chotai, A. (1987). Direct digital and adaptive control by input-output state variable feedback pole assignment. *International Journal of Control*, 46(6):1867–1881.